J Therm Anal Calorim (2010) 101:997–1002
DOI 10.1007/s10973-009-0607-1

Synthesis, crystal structure, and thermodynamics of a high-nitrogen copper complex with *N*, *N*-bis-(1(2)H-tetrazol-5-yl) amine

Bao-Di Xue · Qi Yang · San-Ping Chen · Sheng-Li Gao

Received: 11 October 2009 / Accepted: 17 November 2009 / Published online: 2 December 2009

Abstract A new high-nitrogen complex $[Cu(Hbta)_2]\cdot 4H_2O$ (H_2bta = *N*,*N*-bis-(1(2)H-tetrazol-5-yl) amine) was synthesized and characterized by elemental analysis, single crystal X-ray diffraction and thermogravimetric analyses. X-ray structural analyses revealed that the crystal was monoclinic, space group *P*2(1)/c with lattice parameters $a = 14.695(3)$ Å, $b = 6.975(2)$ Å, $c = 18.807(3)$ Å, $\beta = 126.603(1)°$, $Z = 4$, $D_c = 1.888$ g cm^{-3}, and $F(000) = 892$. The complex exhibits a 3D supermolecular structure which is built up from 1D zigzag chains. The enthalpy change of the reaction of formation for the complex was determined by an RD496–III microcalorimeter at 25 °C with the value of -47.905 ± 0.021 kJ mol^{-1}. In addition, the thermodynamics of the reaction of formation of the complex was investigated and the fundamental parameters *k*, *E*, *n*, $\Delta S^{\theta}_{\neq}$, $\Delta H^{\theta}_{\neq}$, and $\Delta G^{\theta}_{\neq}$ were obtained. The effects of the complex on the thermal decomposition behaviors of the main component of solid propellant (HMX and RDX) indicated that the complex possessed good performance for HMX and RDX.

Keywords Crystal structure · Enthalpy change of the reaction of formation · Thermodynamics · Catalytic thermal decomposition

B.-D. Xue · Q. Yang · S.-P. Chen (✉) · S.-L. Gao (✉)
Key Laboratory of Synthetic and Natural Functional Molecule Chemistry of Ministry of Education, College of Chemistry & Materials Science, Northwest University, Xi'an, Shaanxi 710069, People's Republic of China
e-mail: sanpingchen@126.com

S.-L. Gao
e-mail: gaoshli@nwu.edu.cn

Introduction

Modern high-energy density materials (HEDM) derive most of their energy either (i) from oxidation of the carbon backbone, as with traditional energetic materials [1, 2] or (ii) from their very high positive heat of formation. Nitrogen-rich complexes are new members of the second family and they are environmentally acceptable [3–9]. They rely on their highly efficient gas production and also on their high heat of formation for energy release [10–12], since elemental nitrogen, which of a zero heat of formation, is the major product of decomposition.

H_2bta (*N*,*N*-bis-(1(2)H-tetrazol-5-yl)-amine) is a bidentate chelating ligand with multi-proton donor sites and nitrogen content is 83.43%. It can coordinate to a metal with three reversible types: neutral (H_2bta), monodeprotonated (monoanion, $Hbta^-$), and dideprotonated (dianion, bta^{2-}) types. Friedrich et al. [13] studied the crystal structure and magnetic properties of Cu complex with H_2bta and indicated that H_2bta might serve as components in preparation of a new generation of high performance energetic materials. In order to provide theoretic example for the further application, we are exploring the syntheses, structure characteristics and thermal properties of H_2bta transition metal complexes.

In this article, we reported on the synthesis and structural characterization of $[Cu(Hbta)_2]\cdot 4H_2O$. The thermal stability was investigated by TG-DTG technique. The enthalpy change of the reaction of formation at 25 °C was determined. The thermodynamics of the reaction of formation were investigated, and fundamental parameters are obtained on the basis of reaction thermodynamic and kinetic equations. The effects of the complex on the thermal decomposition behavior of the main component of solid propellant (HMX and RDX) were studied by DSC technique.

Experimental

Materials and measurements

All reagents used for the syntheses were purchased from commercial sources and used without further purification.

Cu^{2+} was determined with EDTA by complexometric titration. C, H and N analyses were carried out using an instrument of Vario EL III CHNOS of Germany. Infrared (IR) spectrum drawn at regular intervals was recorded on a Bruker FTIR instrument as KBr pellets. The TG-DTG analysis was conducted on a P. E. 2100 company thermal analyzer in a static air atmosphere from room temperature to 600 °C. DSC experiment was performed using a CDR-4P thermal analyzer of Shanghai Balance Instrument factory under a flow of 100 mL min^{-1} nitrogen. ICP-AES experiment was carried out on a T.E. IRIS advantage inductively coupled plasma atomic emission spectrophotometer. The calorimetric experiments were performed with an RD496-III type microcalorimeter [14]. The calorimetric constant at 25.15 °C was determined by the Joule effect before experiment, which was 63.901 ± 0.030 μV mW^{-1}. The enthalpy of dissolution of KCl (spectral purity) in deionized water was measured to be 17.238 ± 0.048 kJ mol^{-1}, which was in good agreement with the value of 17.241 ± 0.018 kJ mol^{-1} from reference [15].

The single crystal X-ray experiment was performed on a Bruker Smart Apex CCD diffractometer equipped with graphite monochromatized Mo Kα radiation ($\lambda = 0.71073$ Å) using ω and φ scan mode. The single-crystal structure of complex was solved by direct methods and refined with full-matrix least-squares refinements based on F^2 using SHELXS 97 and SHELXL 97 [16, 17]. All non-H atoms were located using subsequent Fourier-difference methods. In all cases hydrogen atoms were placed in calculated positions and thereafter allowed to ride on their parent atoms. Other details of crystal data, data collection parameters and refinement statistics are given in Table 1. Selected bond distances and bond angles are given in Table 2.

Synthesis of complex

H_2bta was synthesized according to the literature [18].

Synthesis of $[Cu(Hbta)_2]\cdot 4H_2O$: Blue block-like crystal for X-ray diffraction analyses was obtained from the mixture of $Cu(NO_3)_2\cdot 6H_2O$ (0.296 g, 1 mmol), $H_2bta\cdot H_2O$ (0.340 g, 2 mmol) and distilled H_2O (15 mL), which was allowed to evaporate at room temperature for 3 weeks, the complex was filtered and air dried. Yield: 48%. IR (KBr, cm^{-1}) 3425(s), 1622(s), 1588(s), 1448(s), and 1340(s). Anal. Calcd. $C_4H_{12}N_{18}O_4Cu$ weight (%): C, 10.92; H, 2.75; N, 57.33. Found: C, 10.89; H, 2.65; N, 57.25.

Table 1 Crystal data and structure refinement parameters for complex

Empirical formula	$C_4H_{12}N_{18}O_4Cu$
Formula weight	439.86
Crystal system	Monoclinic
Space group	P2(1)/c
a(Å)	14.695(3)
b(Å)	6.975(4)
c(Å)	18.807(3)
α(°)	90
β(°)	126.603(1)
γ(°)	90
V(Å^3)	1547.4(5)
Z	4
ρcalc (g cm^{-3})	1.888
μ(mm^{-1})	1.478
F(000)	892
θ (°)	2.17–25.05
indep reflcn	2,728
Goodness-of-fit on F^2	1.012
Final R indices [I > 2sigma(I)]	$R1 = 0.0408$ $wR2 = 0.1054$
R indices (all data)	$R1 = 0.0608$ $wR2 = 0.1128$
Largest peak and hole (e Å^{-3})	0.494 and −0.604

Table 2 Selected bond lengths (Å) and bond angles (°) for the complex

Cu(1)–N(1)	2.041(3)	Cu(1)–N(9)	1.954(3)
Cu(1)–N(10)	1.960(3)	Cu(1)–N(12)	2.209(3)
Cu(1)–N(18)	2.038(3)		
N(11)–Cu(1)–N(12)	120.4(2)	N(12)–Cu(1)–N(13)	126.7(2)
N(9)–Cu(1)–N(10)	176.3(14)	N(9)–Cu(1)–N(18)	94.52(13)
N(10)–Cu(1)–N(18)	85.58(12)	N(9)–Cu(1)–N(1)	85.73(13)
N(10)–Cu(1)–N(1)	96.96(13)	N(18)–Cu(1)–N(1)	132.0(13)
N(9)–Cu(1)–N(12)	90.78(13)	N(10)–Cu(1)–N(12)	85.97(12)
N(18)–Cu(1)–N(12)	120.0(12)	N(1)–Cu(1)–N(12)	108.0(12)

Results and discussion

Crystal structure of complex

The X-ray structure analysis reveals that the asymmetric unit of the complex consists of one Cu(II) ion, two coordinated $Hbta^-$ and four crystal H_2O molecules. In the unit of $[Cu(Hbta)_2]$, as shown in Fig. 1, four N atoms from two $Hbta^-$ ligand coordinate to the Cu^{2+}. The Cu–N bond lengths are between 1.954 and 2.041 Å. Additionally, one $Hbta^-$ ligand in another $[Cu(Hbta)_2]$ unit connects the Cu^{2+} by one terminal nitrogen atom to form an infinite 1D zigzag chain, as shown in Fig. 2. So, each Cu(II) atom in

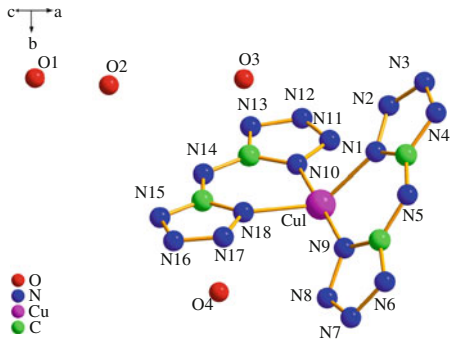

Fig. 1 View of the asymmetric unit of complex. H atoms are omitted for clarity

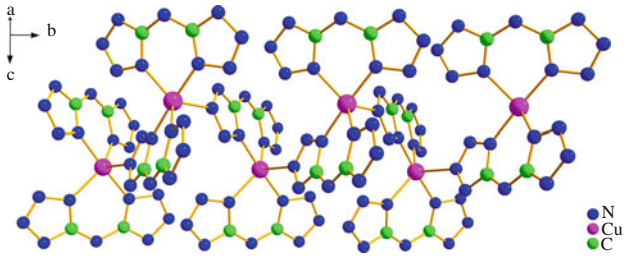

Fig. 2 View of 1D zigzag chain along *b*-axis. H atoms are omitted for clarity

the complex exhibits a distorted square pyramid geometry. The Cu–N bond length is 2.209 Å, which is shorter than the Cu–N bond length 2.269 Å in complex [Cu(bta)$(NH_3)_2{\cdot}H_2O$] and 2.319 Å in complex [Cu(bta)$(NH_3)_2$] [13]. The Cu–Cu separation is found to be 6.116 Å, which is identical to the Cu–Cu separation 6.116 Å in complex [Cu(bta)$(NH_3)_2{\cdot}H_2O$] [13]. The 1D zigzag chain is further extended into a 3D superamolecular network through hydrogen bonds (Table 3) between the crystal waters and nitrogen atom of the $Hbta^-$ ligand, as well as between the crystal waters.

Thermogravimetric analysis

Thermogravimetric analysis (TG-DTG) for the complex was performed from room temperature to 600 °C at a heating rate of 10 °C min^{-1} under a static air atmosphere, as shown in Fig. 3.

The decomposition process of the complex can be divided into three steps. The first step in the range of 40–90 °C was confirmed as the loss of crystal water (observed 15.62%, calcd. 16.39%). It indicated that the water molecules in the title complex were not stable before 90 °C and the special protection measurements should be cautioned during the storage. The second and third steps from 150–400 °C were considered as the break of the $Hbta^-$ ligand and then the complex completely converted

Table 3 Hydrogen bonding interactions in complex

D–H···A	H···A (Å)	D···A (Å)	D–H···A (°)
N(4)–H(4)···N(13)#3	1.93	2.777(4)	168.2
N(5)–H(5)···O(4)#4	1.86	2.698(4)	164.3
N(14)–H(14)···N(6)#5	2.10	2.838(4)	144.3
N(15)–H(15)···O(1)#6	1.84	2.667(4)	160.0
O(1)–H(1B)···N(7)#5	2.06	2.910(4)	159.4
O(3)–H(3A)···N(8)#7	2.20	2.938(5)	164.2
O(4)–H(4B)···O(3)#8	1.96	2.768(5)	158.0
O(4)–H(4A)···N(11)#2	2.25	2.903(4)	134.3
O(4)–H(4A)···N(13)#8	2.67	3.200(5)	122.1
O(3)–H(3B)···N(16)#9	2.15	2.954(5)	163.2
O(1)–H(1A)···O(2)#1	1.92	2.767(7)	178.1

Symmetry transformations: #1 $-x+1$, $y-1/2$, $-z+1/2$; #2 $-x+1, y+1/2, -z+1/2$; #3 $x, -y+1/2, z-1/2$; #4 $x, -y+3/2, z-1/2$; #5 $x, -y+3/2, z+1/2$; #6 $-x, y+1/2, -z+1/2$; #7 $x, y-1, z$; #8 $x, y+1, z$; #9 $-x, -y+1, -z$

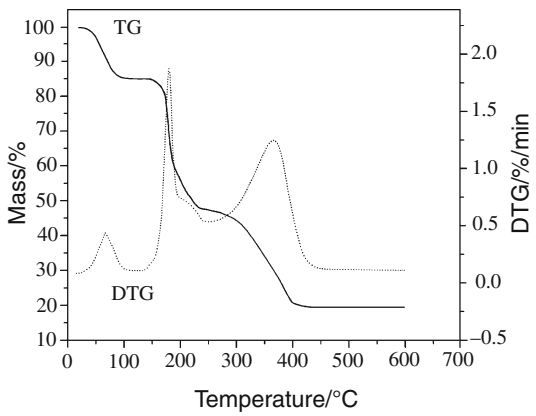

Fig. 3 The TG-DTG curves of the complex at 10 °C min^{-1}

to the remainder CuO with the residual amount of 18.55%, which was in good agreement with the calculated value 18.09%. The remainder CuO was evidenced by X-ray powder diffraction analyses.

Enthalpy change of the reaction of formation

The crude products of the reaction from the calorimetric experiments were collected and separated by the centrifugal effect. The solid crude products were purified and identified as being the same product as the synthesized product. The concentration of Cu^{2+} retained in the centrifugal liquid were determined to be 6×10^{-3} μg mL^{-1} by the ICP-AES experiment, indicating that the starting reactants have been transformed fully to the title product. Within the range of the experimental temperature, the complexation reaction was exothermic. The concentrations of the Cu^{2+} and H_2bta were 0.200 and 0.040 mol L^{-1},

Table 4 Thermokinetic data of the reaction of formation

25 °C			30 °C			35 °C			40 °C		
t/s	H_t/H_0	$10^3 dH_t(dt)^{-1}$/ J s^{-1}	t/s	H_t/H_0	$10^3 dH_t(dt)^{-1}$/ J s^{-1}	t/s	H_t/H_0	$10^3 dH_t(dt)^{-1}$/ J s^{-1}	t/s	H_t/H_0	$10^3 dH_t(dt)^{-1}$/ J s^{-1}
240	0.3095	5.224	285	0.2738	5.916	270	0.3023	6.369	180	0.2212	7.535
255	0.3321	5.054	300	0.2961	5.735	285	0.3221	6.188	195	0.2450	7.306
270	0.3540	4.918	315	0.3179	5.556	300	0.3414	6.011	210	0.2683	7.080
285	0.3755	4.724	330	0.3393	5.382	315	0.3604	5.838	225	0.2912	6.857
300	0.3963	4.567	345	0.3601	5.207	330	0.3789	5.669	240	0.3136	6.641
315	0.4165	4.334	360	0.3804	5.046	345	0.3969	5.504	255	0.3355	6.429
330	0.4361	4.264	375	0.4002	4.881	360	0.4145	5.343	270	0.3568	6.223
345	0.4551	4.119	390	0.4194	4.728	375	0.4316	5.188	285	0.3775	6.022
360	0.4735	3.981	405	0.4380	4.577	390	0.4482	5.034	300	0.3977	5.827
375	0.4914	3.845	420	0.4560	4.377	405	0.4644	4.887	315	0.4172	5.639
390	0.5086	3.699	435	0.4735	4.288	420	0.4801	4.696	330	0.4362	5.406
405	0.5252	3.589	450	0.4905	4.149	435	0.4954	4.604	345	0.4545	5.277
420	0.5413	3.467	465	0.5068	3.984	450	0.5102	4.469	360	0.4723	5.107
435	0.5568	3.349	480	0.5227	3.887	465	0.5245	4.338	375	0.4894	4.940
450	0.5718	3.220	495	0.5380	3.762	480	0.5385	4.210	390	0.5059	4.780
465	0.5862	3.127	510	0.5528	3.642	495	0.5520	4.087	405	0.5219	4.625
480	0.6001	3.021	525	0.5670	3.525	510	0.5651	3.967	420	0.5373	4.477
495	0.6135	2.919	540	0.5808	3.413	525	0.5777	3.852	435	0.5522	4.331
510	0.6265	2.821	555	0.5941	3.305	540	0.5900	3.740	450	0.5665	4.194
525	0.6389	2.727	570	0.6070	3.200	555	0.6019	3.631	465	0.5803	4.061
540	0.6511	2.634	585	0.6193	3.099	570	0.6135	3.526	480	0.5935	3.9321
555	0.6625	2.563	600	0.6313	2.954	585	0.6246	3.423	495	0.6063	3.8081
570	0.6737	2.464	615	0.6428	2.908	600	0.6354	3.324	510	0.6186	3.690
585	0.6844	2.382	630	0.6539	2.817	615	0.6459	3.228	525	0.6304	3.576
600	0.6948	2.303	645	0.6646	2.730	630	0.6561	3.136	540	0.6418	3.465

$H_0 = 3.501$ J (25 °C), 3.096 J (30 °C), 2.757 J (35 °C), 2.369 J (40 °C)

H_0 is the total reaction enthalpy, H_t the reaction heat in a certain time, $dH_t(dt)^{-1}$ the exothermic rate at time t

Table 5 Kinetic and thermodynamic parameters of the reaction of formation

T/°C	K /10^3 s^{-1}	n	r	E/kJ mol^{-1}	ln$A$/s^{-1}	r	$\Delta G^{\theta}_{\neq}$/ kJ mol^{-1}	$\Delta H^{\theta}_{\neq}$/ kJ mol^{-1}	$\Delta S^{\theta}_{\neq}$/ J mol^{-1} s^{-1}	r
25	2.158	0.9986	0.9998	33.21	7.249	0.9990	88.236	30.67	−193.2	0.9988
30	2.637	0.9995	0.9999				89.253			
35	3.310	1.0006	0.9999				90.184			
40	4.082	1.0005	0.9999				91.144			

k the apparent reaction rate constant, A the pre-exponential constant, n the reaction order, r linear correlation coefficient, E apparent activation energy, $\Delta G^{\theta}_{\neq}$ activation Gibbs free energy, $\Delta H^{\theta}_{\neq}$ activation enthalpy, $\Delta S^{\theta}_{\neq}$ activation entropy

respectively. The consumption volumes were 0.4 mL and 2.0 mL, respectively. For reaction (1), Q was measured for six times at 25 °C and the values were −3828.1, −3832.2, −3830.9, −3832.6, −3839.0, and −3831.5 mJ, respectively. The enthalpy change of reaction, $\Delta_r H^{\theta}_m$, was calculated as −47.905 ± 0.021 kJ mol^{-1}. The value of $\Delta_r H^{\theta}_m$ was negative, indicating that it was favorable to the formation of product.

$$Cu^{2+}(aq) + 2Hbta^{-}(aq) \rightarrow Cu(Hbta)_2 \cdot 4H_2O(s) \quad (1)$$

Thermodynamics of the reaction of formation

The solutions collected from each experiment were filtered and the precipitant died. The analytical results identified that the complex had the composition $Cu(Hbta)_2 \cdot 4H_2O(s)$, indicating that the liquid-phase reaction was irreversible.

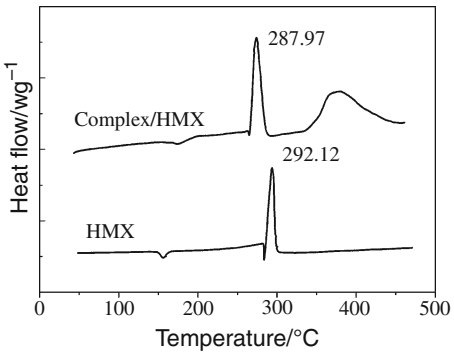

Fig. 4 DSC curves of HMX and mixtures (β = 10 °C min^{-1})

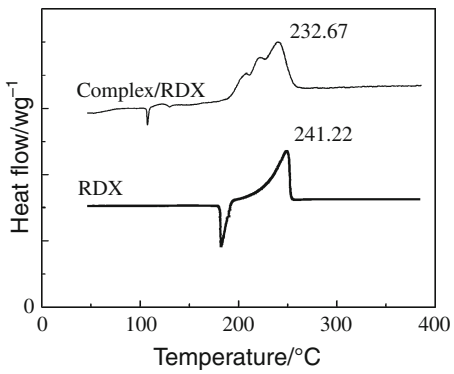

Fig. 5 DSC curves of RDX and mixtures (β = 10 °C min^{-1})

The experimental data were presented in Table 4. The energy change of the reaction system depended on the reaction progression. Based on the thermodynamic equations [19], the thermodynamic parameters and kinetic parameters of the liquid reaction were obtained and listed in the Table 5.

In general, when the apparent activation energy of a reaction was less than 63 kJ mol^{-1}, the reaction proceeded feasibly. Therefore, the reaction (1) was easy to proceed.

The effects of the complex on the thermal decomposition behaviors for HMX and RDX

The DSC curves of each system (complex/the main component of solid propellant, mass ratio 1:3) at heating rate 10 °C min^{-1} were listed in Figs. 4 and 5 and the results were listed in Table 6.

The above results indicated that when the title complex was used together with the main component of solid propellant (HMX and RDX), the peak temperature of thermal decomposition and the activation energy of the mixtures were decreased, respectively, and the decomposition heat was increased [20], showing that the complex accelerated the thermal decomposition of HMX and RDX. The complex possessed good application prospect in the catalytic combustion of HMX and RDX.

Table 6 Thermal decomposition parameters of the main component of solid propellant and mixtures

System	β/°C min^{-1}	T_p/°C	10 °C min^{-1}			E_o/kJ mol^{-1}	E_k/kJ mol^{-1}	ln[A/s^{-1}]
			T_{onset}/°C	ΔT_p/°C	ΔH/J g^{-1}			
HMX	5	287.89	285.86	–	502.21	572.03	592.24	53.84
	10	292.12						
	15	295.82						
	20	297.52						
Complex/HMX	5	283.40	283.71	4.95	1061.84	354.77	363.66	31.99
	10	287.97						
	15	288.21						
	20	289.31						
RDX	5	228.68	220.27	–	588.25	142.67	141.35	12.52
	10	241.22						
	15	243.61						
	20	248.36						
Complex/RDX	5	224.95	219.61	4.50	882.14	115.86	113.35	9.57
	10	232.67						
	15	239.37						
	20	250.26						

β heating rate, T_p maximum peak temperature, E activation energy, ΔH decomposition heat, A pre-exponential constant, subscript "k" for data obtained by kissinger's method; subscript "o" for data obtained by ozawa's method

Conclusions

In summary, we have prepared successfully the title complex. X-ray diffraction analyses indicated that each Cu(II) was five-coordinated in a distorted square pyramid geometry. The complex was thermodecomposed in three steps and then converted to CuO. The reaction enthalpy change of the liquid phase reaction at 25 °C was obtained with the value of -47.905 ± 0.021 kJ mol^{-1}. Based on thermokinetic data of liquid-phase reaction at different temperatures, the thermodynamic parameters and kinetic parameters of the liquid reaction were obtained. DSC experiment revealed that the complex accelerated the thermal decomposition of HMX and RDX. The present study can projected the probable application of the complex in solid propellant field.

Caution

While all hydrates of H_2bta salts are insensitive to shock and friction, the anhydrous H_2bta salts are very sensitive. Safety equipment such as leather gloves, face shields and earplugs are necessary.

Supplementary material

CCDC 695671 contains the supplementary crystallo-graphic data for this paper. These data can be obtained free of charge at http://www.ccdc.ac.uk/conts/retrieving.html or from the Cambridge Crystallographic Data Center (CCDC), 12 Union Road, Cambridge CB21EZ, UK; fax: +44 1223 336033; e-mail: deposit@ccdc.cam.ac.uk.

Acknowledgements We gratefully acknowledge the financial support from the National Natural Science Foundation of China (Grant Nos. 20771089 and 20873100) and the National Natural Science Foundation of Shaanxi Province (Grant Nos. 2007B02 and SJ08B09).

References

1. Feuer H, Nielsen AT. Nitrocompounds: recent advances in synthesis and chemistry. New York: VCH; 1990.
2. Nielsen AT. Nitrocarbons, polycyclic amine chemistry. New York: VCH; 1995.
3. Chavez DE, Hiskey MA, Gilardi RD. 3,3′-azobis(6-amino-1,2,4,5-tetrazine): a novel high-nitrogen energetic material. Angew Chem Int Ed. 2000;39(10):1791–3.
4. Fraenk W, Habereder T, Hammerl A, Klapötke TM, Krumm B, Mayer P, et al. Highly energetic tetraazidoborate anion and boron triazide adducts. Inorg Chem. 2001;40:1334–40.
5. Jones DEG, Armstrong K, Parekunnel T, Kwok QSM. The thermal behavior of BTAw, a high nitrogen fuel. J Therm Anal Calorim. 2006;86:641–9.
6. Klapötke TM, Stierstorfer J, Weber B. New energetic materials: synthesis and characterization of copper 5-nitriminotetrazolates. Inorg Chim Acta. 2009;362:2311–20.
7. Chen SP, Li N, Wei Q, Gao SL (2009) Synthesis, structure analysis and thermodynamics of $[Ni(H_2O)_4(TO)_2](NO3)_2{\cdot}2H_2O$ (TO = 1,2,4-triazole-5-one). J Therm Anal Calorim. doi: 10.1007/s10973-009-0400-1.
8. Yi JH, Zhao FQ, Ren YH, Xu SY, Ma HX, Hu RZ (2009) Thermal decomposition mechanism and quantum chemical investigation of hydrazine 3-nitro-1,2,4-triazol-5-one (HNTO). J Therm Anal Calorim. doi: 10.1007/s10973-009-0416-6.
9. Gavazov K, Lekova V, Boyanov B, Dimitrov A. Some tetrazolium salts and their ion-association complexes with the molybdenum(vi)–4-nitrocatechol anionic chelate DTA and TGA study. J Therm Anal Calorim. 2009;96(1):249–54.
10. Loebbecke S, Schuppler H, Schweikert W. Thermal analysis of the extremely nitrogen-rich solids BTT and DAAT. J Therm Anal Calorim. 2003;72:453–63.
11. Geetha M, Nair UR, Sarwade DB, Gore GM, Asthana SN, Singh H. Studies on CL-20: the most powerful high energy material. J Therm Anal Calorim. 2003;73:913–22.
12. Li N, Chen SP, Gao SL. Crystal structure and thermal analysis of diaquadi 1,2,4-triazole-5-one) Zinc(II) ion nitrate. J Therm Anal Calorim. 2007;89:583–8.
13. Friedrich M, Gálvez-Ruiz JC, Klapötke TM, Mayer P, Weber B, Weigand JJ. BTA copper complexes. Inorg Chem. 2005;44(22):8044–52.
14. Ji M, Liu MY, Gao SL, Shi QZ. The enthalpy of solution in water of complexes of zinc with methionine. Instrum Sci Technol. 2001;29:53–7.
15. Kilday MV. The enthalpy of solution of SRM 1665 (KCl). J Res Natl Inst Stand. 1980;85:467–81.
16. Sheldrick GM. SHELXS-97, program for X-ray crystal structure determination. Germany: Göttingen University; 1997.
17. Sheldrick GM. SHELXL-97, program for X-ray crystal structure refinement. Germany: Göttingen University; 1997.
18. Norris WP, Henry RA. Cyanoguanyl azide chemistry. J Org Chem. 1963;29:650–60.
19. Gao SL, Ji M, Chen SP, Hu RZ, Shi QZ. The thermokinetics of the formation reaction of cobalt histidine complex. J Therm Anal Calorim. 2001;66:423–9.
20. Zhao FQ, Chen P, Li SW, Yin CM, Liu ZR. Effect of the burning rate regulator on the thermal behavior of RDX/AP/HTPB propellant. J Propuls Technol. 2003;1:80–2.